DOI: 10.1002/marc.202000034

Design of pH-degradable polymer-lipid amphiphiles using a ketal-functionalized RAFT chain transfer agent

Jana De Vrieze[1], Simon Van Herck[1], Lutz Nuhn[1,2], Bruno G De Geest[1]

[1]Department of Pharmaceutics, Ghent University, Ghent, Belgium

[2]Max Planck institute for Polymer Research, Mainz, Germany

ABSTRACT

Conjugation of small molecule drug to lipid-polymer amphiphiles is a powerful strategy to alter the pharmacokinetic profile of these molecules by promoting binding to albumin or other serum molecules. Incorporation of a responsive linker between the lipid anchor and the polymer chain could be of interest to avoid indefinite binding of the conjugates to hydrophobic pockets of serum proteins or phospholipid membranes when reaching a target cell or tissue. Here we report on the synthesis of pH-sensitive lipid-polymer conjugates by RAFT polymerisation using a RAFT chain transfer agent that is equipped with a pH-sensitive ketal bond between a cholesterol moiety and the trithiocarbonate RAFT chain transfer group. We demonstrate that in native form these conjugates exhibit high affinity to albumin and cell membranes but loose this ability in response to a mild acidic trigger in aqueous medium.

MANUSCRIPT TEXT

Lipid-polymer amphiphiles are attractive drug carriers owing to their ability to dramatically alter the pharmacokinetic profile of small molecule drugs. Indeed, whereas the latter exhibit fast systemic deposition and renal clearance, lipidation (i.e. conjugation of a lipid motif to the drug molecule of interest) induces binding to serum proteins with hydrophobic binding pockets, such as albumin, which confers a much longer circulation half-life.[1,2] Moreover, intravenous administration of lipid-drug conjugate can result in a higher tumor accumulation due to albumin binding and increased accumulation of albumin in the cancer milieu. In the context of subcutaneous administration, lipid-drug conjugates can form a depot for sustained release or – when properly engineered to be amphiphilic and well-water soluble – can hijack the lymphatic albumin flow and accumulate in lymphoid tissue.[3,4] The latter is of particular interest in view of vaccination and immunotherapy as recently demonstrated by the Irvine group for semi macromolecular drugs such as oligonucleotides and peptides as well as by our group for immune-modulatory small molecule agonists of Toll like receptor 7 (TLR7).[5,6] In these works, lipid amphiphiles were designed by conjugating a lipid motif to the drug molecule through a non-degradable bond. However, for several applications, a system that releases the lipid motif upon cellular internalization could be of benefit, as the lipid motif will tend to anchor to the endosomal phospholipid membrane and, hence, limit accessibility of the drug to trigger a receptor or to be metabolically activated by enzymes.[7]

Therefore, the aim of this work is to design degradable lipid-polymer amphiphiles that can be cleaved off, between the lipid anchor and the hydrophilic polymer in response to a physiological trigger. For this purpose, we made use of a ketal bond which we and others have reported on before to be stable over several days at the physiological pH of 7.4 but can degrade over the time course of several hours under mild acidic conditions such as those found in endosomal intracellular vesicles. Note that effective degradability of drug delivery systems that are equipped with ketal bonds has effectively been shown to occur inside living cells both in vitro and in vivo our recent work. [8,9]

Cholesterol conjugates are known for their spontaneous cell membrane anchoring and albumin-binding properties.[10] Hence, cholesterol was chosen in this work as lipid motif and an acid degradable cholesterol-functionalized trithiocarbonate chain transfer agents (CTAs) for reversible addition-fragmentation chain transfer (RAFT) polymerization was synthesized, according to **Scheme 1**. First, the carboxylate group of cholesteryl hemisuccinate could be activated into an activated ester by carbodiimide-mediated esterification with pentafluorophenol. Next, diamino ketal was covalently attached to the intermediate product **(1)** via amidation reaction of the activated ester group. Note that a large excess of diamino ketal was used to avoid unwanted side products such as the dicholesteryl

ketal derivate. Finally, the remaining primary amine of intermediate product **(2)** was reacted with the pentafluorophenyl-activated 2-propanoic acid butyl trithiocarbonate (PFP-PABTC) to yield the acid sensitive cholesterol-ketal-CTA. As a control we also used an earlier reported CTA where cholesterol was directly conjugate to PABTC through an ester linkage which is stable towards mild acidic conditions compared to the here introduced ketal.[6] These two CTAs will further on be denoted as cholesterol-ketal-CTA and cholesterol-ester-CTA. Successful synthesis was proven by NMR and mass spectroscopy (data shown in Supplementary Information).

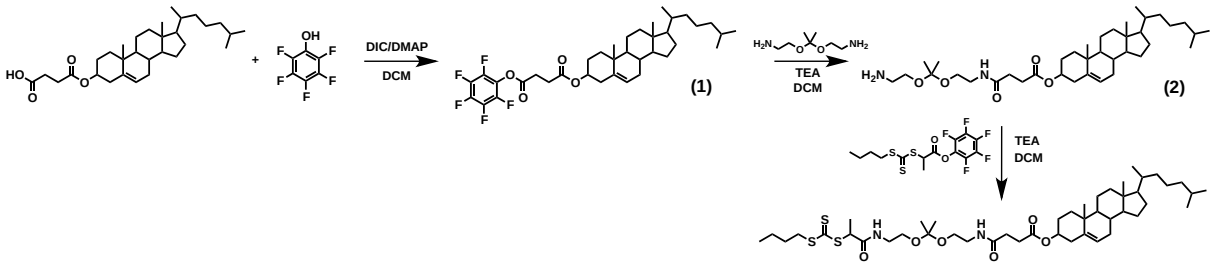

Scheme 1. Synthesis of cholesterol-ketal-CTA.

The respective functionalised CTAs were used for the synthesis of well-defined amphiphile conjugates by RAFT polymerization (**Scheme 2**; exemplified for the cholesterol-ketal-CTA)[11]. Hereto, AIBN was utilized as radical initiator, *N,N*-dimethylacrylamide (DMA) as hydrophilic biocompatible monomer and a degree of polymerization (DP) of 50 was targeted through the monomer to CTA ratio. **Table 1** gives an overview of the polymer characterisation. The polymerization was stopped before completion, which was reflected by low dispersity values < 1.10, indicating a narrow molecular weight distribution as well as high end group fidelity. Consequently, both CTAs provide excellent control over the radical polymerization reaction. To allow monitoring of derived polymers with living cells *in vitro* via fluorescence-based methods, we synthesized rhodamine B labelled copolymers by including acryloxyethyl thiocarbamoyl rhodamine B (ARho) to the monomer mixture. In addition, to achieve a straightforward characterization in solution by diffusion-ordered (DOSY) NMR, we also synthesised a non-amphiphilic polymer based on pentafluorophenylacrylate (PFPA) as monomer using the cholesterol-ketal-CTA (note that the polymer's backbone protons can also individually better be referenced from cholesterol end group protons). For this polymer we aimed at a higher DP to obtain a sufficient decrease in diffusion coefficient between the cholesterol-polymer conjugate and free cholesterol in solution. The properties of these polymers are also shown in **Table 1 and S1**. Note, both ester (cholesterol-ester-CTA) and amide (cholesterol-ketal-CTA) modified RAFT CTAs could be used for

polymerisation of acrylates and acrylamides with high control over the polymerisation, this indicating that modification did not hamper the versatility of the RAFT CTA.

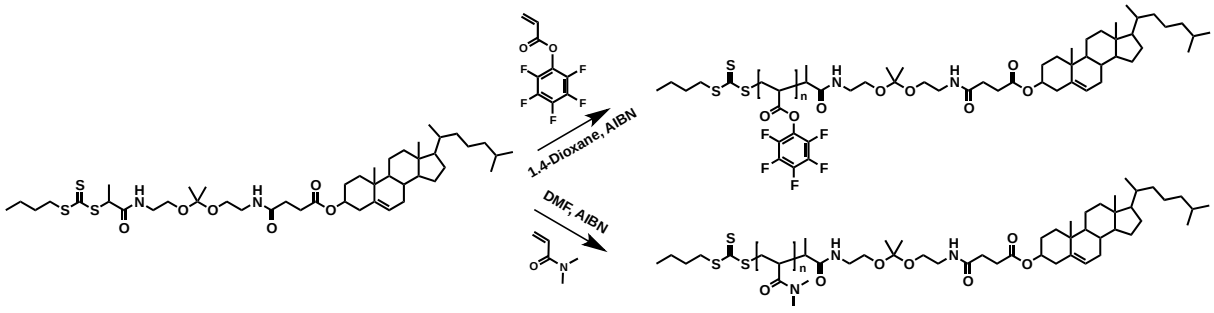

Scheme 2. Synthesis of cholesterol-polymer conjugates via RAFT polymerisation.

Table 1. Characterization of cholesterol-polymers.

Monomer	CTA	M/CTA/AIBN	Conversion [a] (%)	DP [b]	M_n^{Theor} (kDa)[b]	M_n^{SEC} (kDa)	Đ
DMA	Cholesterol-ester-CTA	50/1/0.2	40	20	2.59	4.40 [c]	1.07 [c]
DMA	Cholesterol-ketal-CTA	50/1/0.2	48	24	3.23	4.50 [c]	1.07 [c]
PFPA	Cholesterol-ketal-CTA	105/1/0.2	67	70	17.52	9.23 [d]	1.32 [d]

[a] Determined by ^{1}H NMR analysis. [b] Calculate based on conversion and molecular weight of monomers and CTAs. [c] Determined by SEC in DMAc. [d] Determined by SEC in THF.

Next, we focussed on assessing the degradability of the acid-sensitive ketal-containing conjugates. Due to the ATP-dependent proton pumps, the pH inside endosomes and lysosomes varies from 4.5 to 6.5. Therefore, we chose an intermediate pH of 5.5 to investigate ketal degradation[12]. For comparison, the ester-containing conjugate was used due to the stability of ester group at mild acidic pH. Prior to testing in buffered aqueous media, cholesterol-ketal-poly(PFPA) was analysed by DOSY NMR in aceton (**Figure 1**). After exposure to an acid trigger in the NMR tube (5µL trifluoroacetic acid), a subtle change in diffusion rate of the polymer was observed, compared to the untreated polymer. Importantly, the corresponding cholesterol signals could no longer be observed at the same diffusion rates like the poly(PFPA) signals but shifted to the level of freely soluble cholesterol. These results indicate successful proof of acid-triggered ketal degradation and release of a small molecular cholesterol moiety.

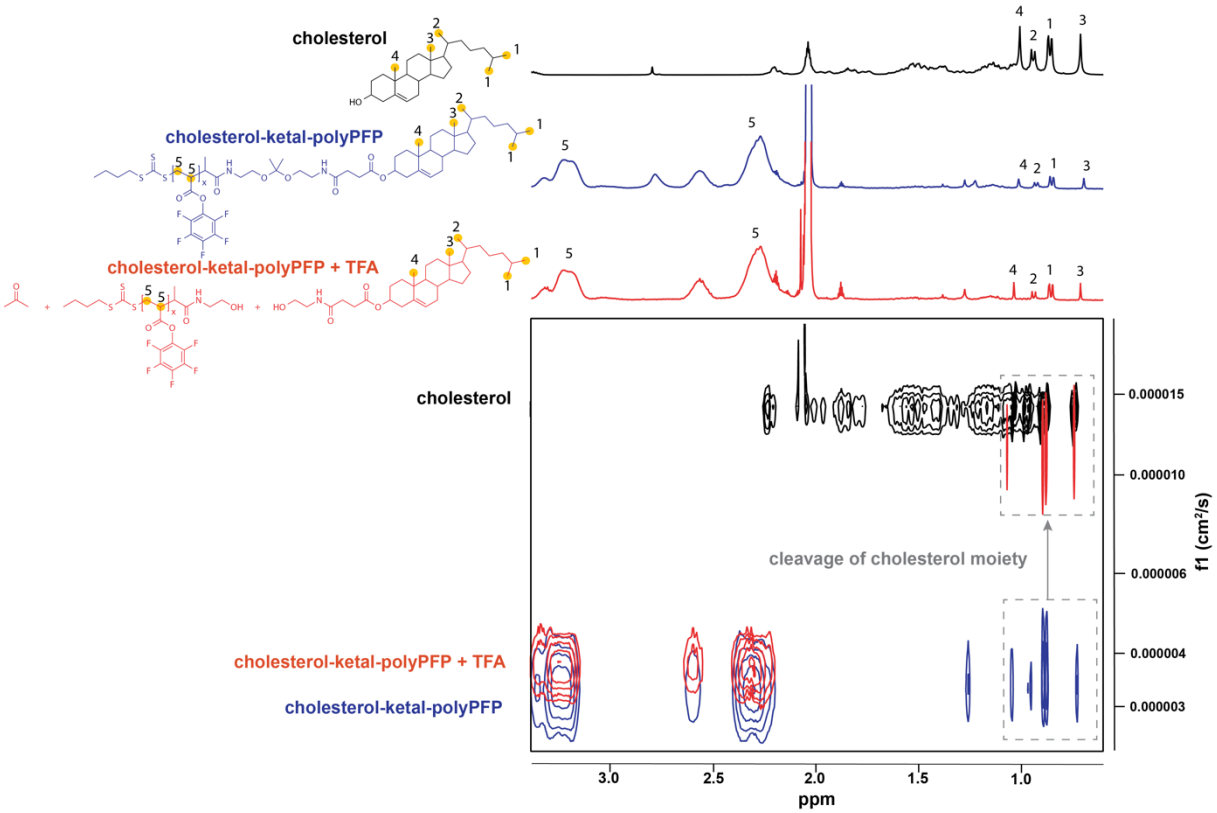

Figure 1. ^{1}H and DOSY NMR (400 MHz, Aceton-D_6) analysis of the degradation of cholesterol-ketal-poly(PFPA) polymer.

Subsequently, the cholesterol-ketal-poly(DMA) conjugates were exposed to acidic conditions. A detailed ^{1}H-NMR analysis of the cholesterol-poly(DMA) polymers demonstrated that the respective ketal (black arrow, **Figure 2**) and the ester group are present after RAFT polymerization (**Figure S12**). However, the ester-containing conjugate remains stable upon exposure to acidic media. Only, the protons from the ketal moiety disappeared upon exposure to acidic conditions (red arrow), indicating successful ketal cleavage at this pH.

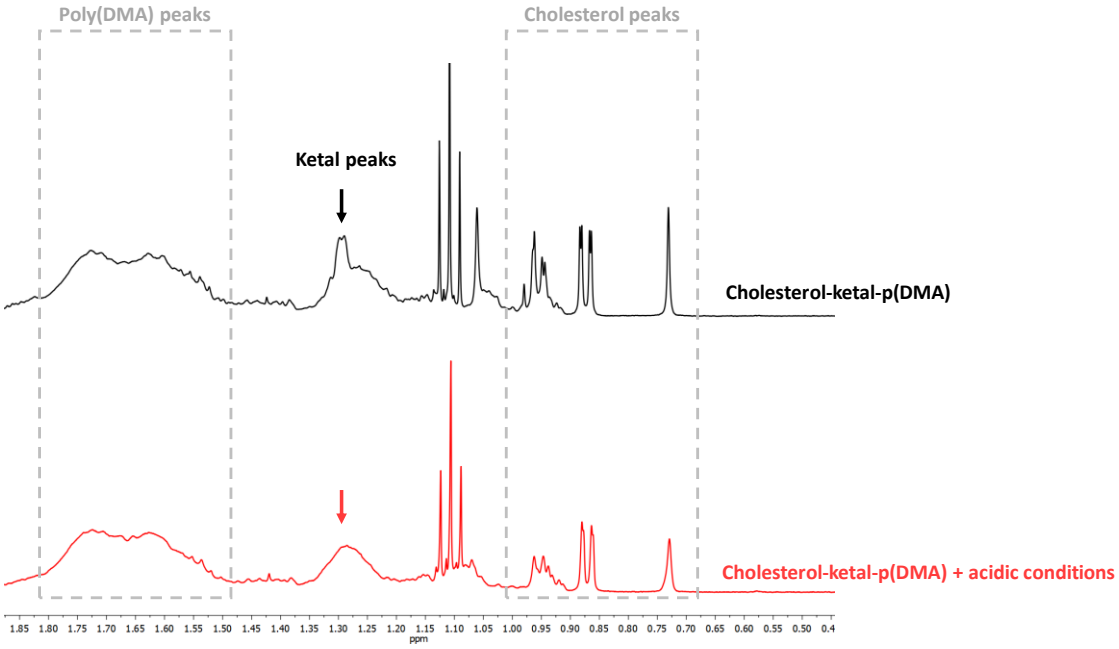

Figure 2. ^{1}H-NMR analysis: a zoomed region of the most relevant peaks before and after exposure to acidic condition.

Using biolayer interferometry (BLI), the binding capacity of the polymers to albumin was investigated. To start, streptavidin sensors were loaded with biotinylated bovine serum albumin (biotin-BSA) and afterwards dipped into solutions containing different concentrations of the respective polymers. **Figure 3** demonstrate strong binding of the cholesterol-ketal-poly(DMA) to BSA-coated sensors. By contrast, this was not the case for the same polymers after removal of the cholesterol moiety by acid treatment. The calculated equilibrium dissociation constant K_D of the intact cholesterol-ketal-poly(DMA) (**table 2**) was about 4-log lower than the K_D of degraded polymer. Curve fitting and calculations emphasize the fact that cholesterol moiety is required for the binding onto albumin-functionalized sensors.

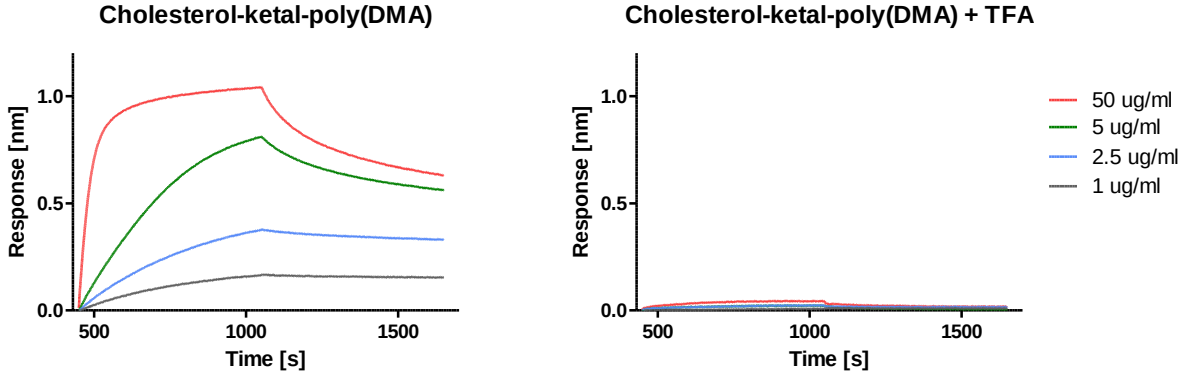

Figure 3. Bio-layer interferometry sensorgrams at different concentrations of cholesterol-ketal-poly(DMA) before and after acid-triggered removal of the cholesterol moiety.

Table 2. Biolayer interferometry experiment: corresponding K_D, $K_{D\ error}$, and R^2 values.

Sample	R^2	K_D	$K_{D\ error}$
Cholesterol-ketal-poly(DMA)	0.9987	$1.452 * 10^{-10}$	$2.525 * 10^{-10}$
Cholesterol-ketal-poly(DMA) + TFA	0.9696	$1.757 * 10^{-6}$	$4.596 * 10^{-8}$

Owing to our interest in immune-engineering and the use of amphiphile carriers for targeting immune cells in lymphoid tissue, we investigated the interaction between the cholesterol-polymer conjugates and DC 2.4 cells (immortalize mouse dendritic cells). The cells were pulsed with fluorescently labelled conjugates at 4 °C and 37 °C, followed by washing to remove unbound polymer and the cellular association was quantified by flow cytometry. Note that at 4 °C active energy-dependent endocytosis is blocked and mere membrane anchoring due to insertion of the cholesterol moiety into the phospholipid bilayer cell membrane is expected to occur.

Flow cytometry analysis (**Figure 4**) at 4 °C shows that the mean fluorescence intensity of the cells treated with fluorescently labelled poly(DMA/ARho) lacking a cholesterol moiety (i.e. obtained by acid-based hydrolysis of cholesterol-ketal-poly(DMA/ARho) is within the same range as the autofluorescence of untreated cells. By contrast, cells pulsed cholesterol-ketal-poly(DMA/ARho) show clear cellular association. These findings indicate that a cholesterol-group is required to anchor to the cell membrane. Consequently, the ability of the cholesterol moiety to mediate cellular association at 4 °C is translated into highly efficient cellular uptake of the conjugates at 37 °C.

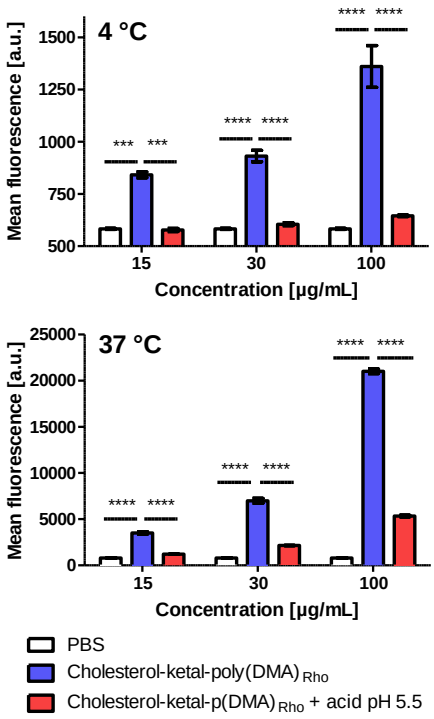

Figure 4. Flow cytometry analysis of DC 2.4 pulsed at 4 °C and 37 °C with cholesterol-poly(DMA) before and after degradation of ketal-moiety (t-test: ****: < 0.0001; ***: <0.001).

Confocal microscopy at 37°C (**Figure 5A**) provides visual proof that cholesterol-ketal-poly(DMA/ARho) conjugates become well internalised by the cell, showing dotted pattern of intracellular fluorescence which likely originates from accumulation in endosomal vesicles. By contrast, a much lower extend of intracellular fluorescence is observed in case of cells pulsed with poly(DMA/ARho) lacking a cholesterol moiety. To provide further proof that cholesterol-ketal-poly(DMA/Rho) can anchor to the phospholipid bilayer cell membrane, we pulsed cells with cholesterol-ketal-poly(DNA/Rho) and poly(DMA/Rho) and imaged cell uptake in real time by confocal microscopy (**Figure 5B**). These experiments indicated that during cell uptake, cholesterol-ketal-poly(DMA/Rho) effectively anchors to the cell membrane, which could not be detected for conjugates that lack a cholesterol moiety.

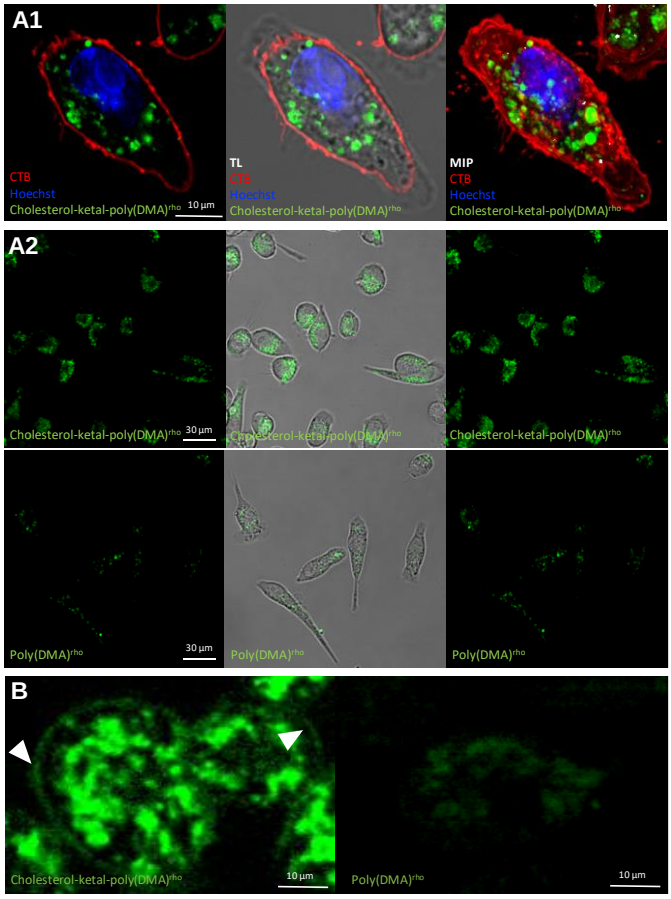

Figure 5. Confocal microscopy experiment on DC 2.4 of fluorescently labelled polymers. (**A1**) Overnight incubation of cholesterol-ketal polymer at 37 °C with nucleus and membrane staining (left: confocal image – middle: overlay with DIC channel – right: maximum intensity projection). (**A2**) Overnight incubation of cholesterol-ketal polymer and cholesterol-ester polymer at 37 °C (left: confocal image – middle: overlay with DIC channel – right: maximum intensity projection) (**B**) Realtime live cell imaging of cellular uptake for both polymers.

Summarizing, we have reported in this work on pH-sensitive cholesterol-polymer conjugates that release the cholesterol moiety upon exposure to mildly acidic pH. This was accomplished by inserting a ketal bond between cholesterol and a chain transfer agent for RAFT polymerization. This was used to grow a polymer chain from cholesterol fused via an pH responsive group. NMR analysis gave proof of the pH-dependent degradability of the ketal bond in solution. Biolayer interferometry, flow cytometry and confocal microscopy provided proof that interaction with albumin or phospholipid cell membranes as well as cellular uptake strongly depends on the presence of the cholesterol moiety. Hence, we believe that this polymer design could be used for fabrication of drug-conjugates that take full advantage of serum protein-binding and cell membrane-binding properties, but release their cholesterol anchor in response to mild acidic pH values such as those found in endosomes as well as in the tumor microenvironment.

References

1. Nuhn, L. *et al.* PH-degradable imidazoquinoline-ligated nanogels for lymph node-focused immune activation. *Proc. Natl. Acad. Sci. U. S. A.* **113**, 8098–8103 (2016).

2. Kim, E. *et al.* In vivo characterization of the physicochemical properties of TLR agonist delivery that enhance vaccine immunogenicity. *Nat. Biotechnol.* **33**, 1201–1210 (2015).

3. Zheng, Y. R. *et al.* Pt(IV) prodrugs designed to bind non-covalently to human serum albumin for drug delivery. *J. Am. Chem. Soc.* **136**, 8790–8798 (2014).

4. Wolfrum, C. *et al.* Mechanisms and optimization of in vivo delivery of lipophilic siRNAs. *Nat. Biotechnol.* **25**, 1149–1157 (2007).

5. Liu, H. *et al.* Structure-based Programming of Lymph Node Targeting in Molecular Vaccines. **507**, 519–522 (2014).

6. De Vrieze, J. *et al.* Potent lymphatic translocation and spatial control over innate immune activation by polymer-lipid amphiphile conjugates of small molecule TLR7/8 agonists. *Angew. Chemie* **131**, 15535–15541 (2019).

7. Wu, T. Y. H. *et al.* Rational design of small molecules as vaccine adjuvants. *Sci. Transl. Med.* **6**, 1–13 (2014).

8. Binauld, S. & Stenzel, M. H. Acid-degradable polymers for drug delivery: A decade of innovation. *Chem. Commun.* **49**, 2082–2102 (2013).

9. Lee, I. *et al.* Ketal containing amphiphilic block copolymer micelles as pH-sensitive drug carriers. *Int. J. Pharm.* **448**, 259–266 (2013).

10. Elliot C. Woods, Nathan A. Yee, Jeff Shen, C. R. B. Glycocalyx Engineering with a Recycling Glycopolymer that Increases Cell Survival in vivo. *Angew. chemie* 15782–15788 (2015).

11. Boyer, C. *et al.* Bioapplications of RAFT polymerization. *Chem. Rev.* **109**, 5402–5436 (2009).

12. Hu, Y. B., Dammer, E. B., Ren, R. J. & Wang, G. The endosomal-lysosomal system: From acidification and cargo sorting to neurodegeneration. *Transl. Neurodegener.* **4**, 1–10 (2015).

13. Vanparijs, N. *et al.* Polymer-protein conjugation via a 'grafting to' approach-a comparative study of the performance of protein-reactive RAFT chain transfer agents. *Polym. Chem.* **6**, 5602–5614 (2015).

14. Van Herck, S. *et al.* Water-soluble withaferin A polymer prodrugs via a drug-functionalized

RAFT CTA approach. *Eur. Polym. J.* **110**, 313–318 (2019).

15. Eberhardt, M., Mruk, R., Zentel, R. & Théato, P. Synthesis of pentafluorophenyl(meth)acrylate polymers: New precursor polymers for the synthesis of multifunctional materials. *Eur. Polym. J.* **41**, 1569–1575 (2005).

SUPPORTING INFORMATION

Materials and Methods

Materials

Unless otherwise noted, all chemicals and solvents were obtained from commercial sources. The RAFT-CTA 2- propanoic acid butyl trithiocarbonate (PABTC), cholesterol-ester-CTA and PFP-PABTC-CTA were synthesized according to literature[6,13,14]. Cholesteryl hemisuccinate was purchased from Sigma Aldrich. 2,2'-azobis(2-methylpropionitrile) (AIBN) was purified by recrystallization from diethyl ether prior use as initiator. The monomer *N,N*-dimethylacrylamide (DMA) was purified over an inhibitor remover column and pentafluorophenyl acrylate (PFPA) was synthesized as reported in literature[15]. Acryloxyethyl thiocarbamoyl rhodamine B (ARho) was obtained from polysciences. DC 2.4 cell line was a kind gift from Dr. Kenneth Rock (University of Massachusetts, Boston, US). Cell culture medium and supplements were purchased from Life Technologies.

Instrumentation

All ^{1}H-, ^{13}C-, ^{19}F- and 2D-NMR spectra were recorded on a Bruker 400 MHz FT NMR spectrometer. Chemical Shifts (δ) were provided in ppm relative to TMS. Samples were prepared in $CDCl_3$ or CD_3OD. Their signals were referenced to residual nondeuterated NMR solvent signals. ESI-mass spectrometry (ESI-MS) was performed on a Waters LCT Premier XE Time of flight (TOF) equipped with an electrospray Ionization and coupled to a Waters Alliance HPLC system. Size exclusion chromatography (SEC) was performed on a Shimadzu 20A system in *N,N*-dimethylacetamide (DMAc) containing 50 mM LiBr or tetrahydrofuran (THF) as solvent. The system was equipped with a 20A ISO-pump and a 20A refractive index detector (RID). Measurements were recorded at 50 °C with a flow rate of 0.700 mL/min for DMAc-SEC. For THF-SEC a flow rate of 1.00 mL/min was applied at room temperature. Calibration of the 2 PL 5 µm mixed-D columns was done with poly(methyl methacrylate) standards for DMAc-SEC or poly(styrene)standard for THF-SEC, both obtained from Polymer Standard Services (Mainz, Germany). All samples were run with toluene as an internal standard and at a concentration of 5 mg/mL. Bio-layer interferometry was performed on a FortéBio Octet® RED96 system. For all experiments, streptavidin coated sensors were used (Pall FortéBio) together with black flat bottom 96 well plates (Greiner). Confocal microscopy images were recorded on a Leica DMI6000 B inverted microscope equipped with an oil immersion objective (Leica, 63 x, NA 1.40) and attached to an Andor DSD2 confocal scanner.

Images were processed using the ImageJ software package. Flow cytometry analysis (FACS) was performed using a BD Accuri C6 (BD Biosciences) and data was processed using FlowJo software package.

Synthesis cholesterol-ketal-CTA

First, a round bottom flask was filled with cholesteryl hemisuccinate (2.0 g, 4.109 mmol), pentafluorophenol (832.0 mg, 4.519 mmol) and 4-(dimethylamino)pyridine (50.2 mg, 0.411 mmol). All compounds were dissolved in 40 mL anhydrous dichloromethane (DCM) and cooled on ice. Subsequently, a solution of N,N'-diisopropylcarbodiimide (699.9 µL, 4.519 mmol) in anhydrous DCM was added dropwise to the stirring reaction mixture. After 1 h ice bad was removed and the mixture was stirred overnight at room temperature. The mixture was concentrated and purified by column chromatography (95:5 hexane: ethyl acetate) (yield 92.5 %). The purified compound **intermediate 1** was characterized by NMR.

^{1}H-NMR (400 MHz, $CDCl_3$, **Figure S1 cholesteryl hemisuccinate**) δ (ppm): 5.36 – 5.24 (m, 1H, -C=C**H**-CH_2-); 4.66 – 4.49 (m, 1H, -(C=O)-O-C**H**-CH_2-C-); 2.68 – 2.48 (m, 4H, -(C=O)-(C**H$_2$**)$_2$-(C=O)-); 2.25 (d, *J* = 7.9 Hz, 2H, -(C=O)-O-CH-C**H$_2$**-C-); 2.02 – 1.85 (m, 2H, -C=CH-C**H$_2$**-CH-CH-); 0.95 (s, 3H, -O-CH-$(CH_2)_2$-C-(C**H$_3$**)-CH-); 0.84 (d, *J* = 6.5 Hz, 3H, -C_5H_6-CH-(C**H$_3$**)-$(CH_2)_3$-CH-$(CH_3)_2$); 0.80 (dd, *J* = 6.6, 1.3 Hz, 6H, -C_5H_6-CH-(CH_3)-$(CH_2)_3$-CH-(C**H$_3$**)$_2$); 0.61 (s, 3H, -C_6H_7-C-(C**H$_3$**)-C_5H_6-). APT ^{13}C NMR (101 MHz, $CDCl_3$, **Figure S2 cholesteryl hemisuccinate**) δ (ppm): 177.99 (HO-(**C**=O)-CH_2-); 171.99 (HO-(C=O)-$(CH_2)_2$-(**C**=O)-O-CH-); 140.00 (-(C=O)-O-CH-CH_2-**C**=CH-); 123.35 (-C=**C**H-CH_2-CH-CH-); 75.22 (-(C=O)-O-**C**H-CH_2-C-); 57.16 – 56.61 (-C_6H_7-**C**H-$(CH_2)_2$-**C**H-CH-(CH_3)-$(CH_2)_3$-CH-$(CH_3)_2$); 50.48 (-O-CH-$(CH_2)_2$-C-**C**H-); 42.78 (-$(CH_2)_2$-C-CH-$(CH_2)_2$-**C**-(CH_3)-CH-); 38.48 (-(C=O)-O-CH-**C**H_2-C-); 37.42 (-O-CH-$(CH_2)_2$-**C**-CH-); 36.26 (-C_5H_6-**C**H-(CH_3)-CH_2-); 32.32 (-C=CH-CH_2-**C**H-); 32.37 (-C=CH-**C**H_2-CH-); 29.70 - 29.39 (HO-(C=O)-**C**H_2-**C**H_2-(C=O)-O-); 28.48 (-$(CH_2)_3$-**C**H-$(CH_3)_2$); 23.27 – 23.04 (-$(CH_2)_3$-CH-(**C**H_3)$_2$); 19.78 (-O-CH-$(CH_2)_2$-C-(**C**H_3)-CH-); 19.19 (-C_5H_6-CH-(**C**H_3)-$(CH_2)_3$-CH-$(CH_3)_2$); 12.36 (-C_6H_7-C-(**C**H_3)-C_5H_6-).

^{1}H NMR (400 MHz, $CDCl_3$, **Figure S3 intermediate 1**) δ (ppm): 5.41 – 5.33 (m, 1H, -C=C**H**-CH_2-); 4.73 – 4.59 (m, 1H, -(C=O)-O-C**H**-CH_2-C-); 3.04 – 2.95 (m, 2H, -(C=O)-C**H$_2$**-CH_2-(C=O)-); 2.80 – 2.69 (m, 2H, -(C=O)-CH_2-C**H$_2$**-(C=O)-); 2.37 – 2.28 (m, 2H, -(C=O)-O-CH-C**H$_2$**-C-); 2.05 – 1.93 (m, 2H, -C=CH-C**H$_2$**-CH-CH-); 1.02 (s, 3H, -O-CH-(CH2)2-C-(C**H$_3$**)-CH-); 0.91 (d, *J* = 6.5 Hz, 3H, -C_5H_6-CH-(C**H$_3$**)-$(CH_2)_3$-CH-$(CH_3)_2$); 0.86 (dd, *J* = 6.6, 1.4 Hz, 6H, -C_5H_6-CH-(CH_3)-$(CH_2)_3$-CH-(C**H$_3$**)$_2$); 0.68 (s, 3H, -C_6H_7-C-(C**H$_3$**)-C_5H_6-). APT ^{13}C NMR (101 MHz, $CDCl_3$, **Figure S4 intermediate 1**) δ (ppm): 170.84 (-(C=O)-$(CH_2)_2$-(**C**=O)-O-CH-); 168.63 (C_6F_5-O-(**C**=O)-CH_2-); 141.35 – 138.89 (**C**$_6F_5$-O-); 138.89 (-(C=O)-O-CH-CH_2-**C**=CH-); 122.92 (-C=**C**H-CH_2-CH-CH-

); 75.00 (-(C=O)-O-**C**H-CH_2-C-); 56.90 – 56.32 (-C_6H_7-**C**H-$(CH_2)_2$-**C**H-CH-(CH_3)-$(CH_2)_3$-CH-$(CH_3)_2$); 50.19 (-O-CH-$(CH_2)_2$-C-**C**H-); 42.51 (-$(CH_2)_2$-C-CH-$(CH_2)_2$-**C**-(CH_3)-CH-); 38.11 (-(C=O)-O-CH-**C**H_2-C-); 37.12 (-O-CH-$(CH_2)_2$-**C**-CH-); 34.77 (-C_5H_6-**C**H-(CH_3)-CH_2-); 32.04 (-C=CH-**C**H_2-CH-); 30.83 (-C=CH-CH_2-**C**H-); 28.67 (C_6F_5-O-(C=O)-CH_2-**C**H_2-(C=O)-O-); 28.37 (C_6F_5-O-(C=O)-**C**H_2-CH_2-(C=O)-O-); 27.00 (-$(CH_2)_3$-**C**H-$(CH_3)_2$); 22.97 – 22.71 (-$(CH_2)_3$-CH-(**C**$H_3)_2$); 19.42 (-O-CH-$(CH_2)_2$-C-(**C**H_3)-CH-); 18.95 (-C_5H_6-CH-(**C**H_3)-$(CH_2)_3$-CH-$(CH_3)_2$); 12.06 (-C_6H_7-C-(**C**H_3)-C_5H_6-). ^{19}F NMR (471 MHz, $CDCl_3$, **Figure S5 intermediate 1**) δ (ppm): -152.07 – -153.03 (m, 2F, **o**-C_6**F**$_5$-); -157.88 (t, *J* = 22.0 Hz, 1F, **p**-C_6**F**$_5$-); -162.14 – -162.37 (m, 2F, **m**-C_6**F**$_5$-).

Next, 2,2-bis(aminoethoxy)propane (800.0 µL, 5.020 mmol) and triethylamine (TEA) (700.2 µL, 5.020 mmol) were dissolved in 40 mL anhydrous DCM under inert atmosphere. The mixture was cooled to 0°C and a solution of the purified compound of step 1 (1.1 g, 1.673 mmol, dissolved in 3 mL anhydrous DCM) was added dropwise while vigorously stirring. After overnight stirring, the crude mixture was concentrated under reduced pressure and purified by column chromatography (95:5 DCM:methanol + 0.5% ammonium hydroxide) (yield 80.0%). The **product intermediate 2** was analysed by NMR and MS.

^{1}H NMR (400 MHz, CD_3OD, **Figure S6 intermediate 2**) δ (ppm): 5.41 (d, *J* = 4.9 Hz, 1H, -C=C**H**-CH_2-); 4.61 – 4.51 (m, 1H, -(C=O)-O-C**H**-CH_2-C-); 3.56 – 3.47 (m, 4H, H_2N-CH_2-C**H$_2$**-O-C-$((CH_3)_2)$-O-C**H$_2$**-CH_2-NH-); 3.37 – 3.34 (m, 2H, H_2N-CH_2-CH_2-O-C-$((CH_3)_2)$-O-CH_2-C**H$_2$**-NH-); 2.89 – 2.83 (m, 2H, H_2N-C**H$_2$**-CH_2-O-C-$((CH_3)_2)$-O-CH_2-CH_2-NH-); 2.63 – 2.56 (m, 2H, -NH-(C=O)-C**H$_2$**-CH_2-(C=O)-); 2.53 – 2.46 (m, 2H, -NH-(C=O)-CH_2-C**H$_2$**-(C=O)-); 2.34 (d, *J* = 9.0, 3.2 Hz, 2H, -(C=O)-O-CH-C**H$_2$**-C-); 2.12 – 1.99 (m, 2H, -C=CH-C**H$_2$**-CH-CH-); 1.38 (s, 6H, -O-C-$((C\mathbf{H_3})_2)$-O-); 1.07 (s, 3H, -O-CH-$(CH_2)_2$-C-(C**H$_3$**)-CH-); 0.97 (d, *J* = 6.6 Hz, 3H, -C_5H_6-CH-(C**H$_3$**)-$(CH_2)_3$-CH-$(CH_3)_2$); 0.90 (dd, *J* = 6.6, 1.5 Hz, 6H, -C_5H_6-CH-(CH_3)-$(CH_2)_3$-CH-(C**H$_3$**)$_2$); 0.75 (s, 3H, -C_6H_7-C-(C**H$_3$**)-C_5H_6-). APT ^{13}C NMR (101 MHz, $CDCl_3$, **Figure S7 intermediate 2**) δ (ppm): 174.50 (-NH-(**C**=O)-$(CH_2)_2$-(C=O)-O-CH-); 173.79 (-NH-(C=O)-$(CH_2)_2$-(**C**=O)-O-CH-); 141.14 (-(C=O)-O-CH-CH_2-**C**=CH-); 123.69 (-C=**C**H-CH_2-CH-CH-); 101.48 (NH_2-$(CH_2)_2$-O-**C**-$((CH_3)_2)$-O-CH_2-); 75.71 (-(C=O)-O-**C**H-CH_2-C-); 62.04 – 60.63 (NH_2-CH_2-**C**H_2-O-C-$((CH_3)_2)$-O-**C**H_2-CH_2-NH-); 58.14 – 57.57 (-C_6H_7-**C**H-$(CH_2)_2$-**C**H-CH-(CH_3)-$(CH_2)_3$-CH-$(CH_3)_2$); 51.64 (-O-CH-$(CH_2)_2$-C-**C**H-); 43.53 (-$(CH_2)_2$-C-CH-$(CH_2)_2$-**C**-(CH_3)-CH-); 42.19 (NH_2-**C**H_2-CH_2-O-); 41.13 (NH_2-$(CH_2)_2$-O-C-$((CH_3)_2)$-O-CH_2-**C**H_2-NH-); 39.12 (-(C=O)-O-CH-**C**H_2-C-); 37.77 (-O-CH-$(CH_2)_2$-**C**-CH-); 33.02 (-C=CH-**C**H_2-CH-CH-); 31.36 (-NH-(C=O)-CH_2-**C**H_2-(C=O)-O-); 30.64 (-NH-(C=O)-**C**H_2-CH_2-(C=O)-O-); 25.15 (NH_2-$(CH_2)_2$-O-C-$((\mathbf{C}H_3)_2)$-O-CH_2-CH_2-NH-); 23.21 – 22.96 (-C_5H_6-CH-(CH_3)-$(CH_2)_3$-CH-(**C**$H_3)_2$); 19.77 (-O-CH-$(CH_2)_2$-C-(**C**H_3)-CH-); 19.28 (-C_5H_6-CH-(**C**H_3)-$(CH_2)_3$-CH-$(CH_3)_2$); 12.34 (-C_6H_7-C-(**C**H_3)-C_5H_6-).

ESI-MS (**Figure S8**) : m/z $[M+H]^+$ = 631.5073 (theoretical); found = 631.4977

$[M+Na]^+$ = 653.4892 (theoretical); found = 653.4891

$[M+K]^+$ = 669.4632 (theoretical); found = 669.4615

Finally, PFP-PABTC (1.6 g, 3.900 mmol) was dissolved in anhydrous DCM (9 mL) into a round bottom flask and placed under inert atmosphere on ice. To this vigorously stirred solution, a mixture of the obtained **intermediate 2** (0.82 g, 1.300 mmol) and TEA (543.4 µL, 3.900 mmol) in 2 mL dry DCM was added dropwise. Afterwards, the solution was placed at room temperature and left stirring overnight. The synthesized product was purified by column chromatography using a gradient (from 70:30 hexane: EtOAc + 1% TEA to 50:50 hexane: EtOAc + 1% TEA) (yield 90%). The product **cholesterol-ketal-CTA** was analysed by NMR and MS.

^{1}H NMR (400 MHz, CD_3OD, **Figure S9 Cholesterol-ketal-CTA**) δ (ppm): 5.41 – 5.36 (m, 1H, -C=C**H**-CH_2-); 4.59 – 4.49 (m, 1H, -(C=O)-O-C**H**-CH_2-C-); 3.50 – 3.33 (m, 8H, -(C=O)-NH-(C**H₂**)$_2$-O-C-((CH_3)$_2$)-O-(C**H₂**)$_2$-NH-(C=O)-); 2.61 – 2.55 (m, 2H, -NH-(C=O)-C**H₂**-CH_2-(C=O)-); 2.52 – 2.45 (m, 2H, -NH-(C=O)-CH_2-C**H₂**-(C=O)-); 2.35 – 2.29 (m, 2H, -(C=O)-O-CH-C**H₂**-C-); 2.11 – 2.00 (m, 2H, -C=CH-C**H₂**-CH-CH-); 1.56 – 1.54 (d, *J* = 7.33 Hz, 3H, -S-CH-(C**H₃**)-(C=O)-); 1.34 – 1.32 (m, 6H, -O-C-((C**H₃**)$_2$)-O-); 1.05 (s, 3H, -O-CH-(CH_2)$_2$-C-(C**H₃**)-CH-); 0.97 – 0.93 (m, 6H, -C_5H_6-CH-(C**H₃**)-(CH_2)$_3$-CH-(CH_3)$_2$ + C**H₃**-((CH_2)$_3$)-S-); 0.88 (dd, *J* = 6.6, 1.5 Hz, 6H, -C_5H_6-CH-(CH_3)-(CH_2)$_3$-CH-(C**H₃**)$_2$); 0.72 (s, 3H, -C_6H_7-C-(C**H₃**)-C_5H_6-). APT ^{13}C NMR (101 MHz, $CDCl_3$, **Figure S10 Cholesterol-ketal-CTA**) δ (ppm): 174.39 (-NH-(**C**=O)-(CH_2)$_2$-(C=O)-O-CH-); 173.81 (-NH-(C=O)-(CH_2)$_2$-(**C**=O)-O-CH-); 173.00 (-S-CH-(CH_3)-(**C**=O)-NH-); 141.02 (-(C=O)-O-CH-CH_2-**C**=CH-); 123.64 (-C=**C**H-CH_2-CH-CH-); 101.34 (NH_2-(CH_2)$_2$-O-**C**-((CH_3)$_2$)-O-CH_2-); 75.61 (-(C=O)-O-**C**H-CH_2-C-); 60.63 – 60.22 (-NH-CH_2-**C**H_2-O-C-((CH_3)$_2$)-O-**C**H_2-CH_2-NH-); 58.05 – 57.53 (C_6H_7-**C**H-(CH_2)$_2$-**C**H-CH-(CH_3)-CH_2-); 51.55 (-O-CH-(CH_2)$_2$-C-**C**H-); 50.59 (-S-**C**H-(CH_3)-(C=0)-); 38.23 (-O-CH-**C**H_2-C-); 37.05 (-C_5H_6-**C**H-(CH_3)-); 33.19 (-C=CH-CH_2-**C**H-); 33.01 (-C=CH-**C**H_2-CH-); 31.38 (-NH-(C=O)-CH_2-**C**H_2-(C=O)-O-); 31.27 (-NH-(C=O)-**C**H_2-CH_2-(C=O)-O-); 29.14 (-(CH_2)$_3$-**C**H-(CH_3)$_2$); 25.29 (-NH-(CH_2)$_2$-O-C-((**C**H_3)$_2$)-O-CH_2-CH_2-NH-); 23.04 – 22.94 (-C_5H_6-CH-(CH_3)-(CH_2)$_3$-CH-(**C**H_3)$_2$); 19.80 (-O-CH-(CH_2)$_2$-C-(**C**H_3)-CH-); 19.25 (-C_5H_6-CH-(**C**H_3)-(CH_2)$_3$-CH-(CH_3)$_2$); 17.90 (-S-CH-(**C**H_3)-(C=O)-); 13.93 (**C**H_3-(CH_2)$_3$-S-); 12.33 (-C_6H_7-C-(**C**H_3)-C_5H_6-).

ESI-MS (**Figure S11**) : m/z $[M+H]^+$ = 851.5073 (theoretical); found = 851.5098

$[M+Na]^+$ = 873.4892 (theoretical); found = 873.4922

$[M+K]^+$ = 889.4632 (theoretical); found = 889.4661

RAFT polymerization

The purified monomer DMA (113.0 mg, 1.14 mmol), cholesterol-ketal-CTA (19.4 mg, 0.023 mmol) and initiator AIBN (0.75 mg, 0.005 mmol) were dissolved in 0.5 mL anhydrous *N,N*-dimethylformamide (DMF) in a Schlenk tube equipped with a stir bar. The solution was degassed by five freeze-vacuum-thaw cycles and afterwards the Schlenk tube was placed in a preheated oil bath of 70 °C. After 2 h, the polymerization was stopped and the polymer was purified by threefold precipitation in ice cold diethyl ether. The polymer was dried under vacuum. Monomer conversion was calculated by ^{1}H-NMR of the reaction mixture and the polymer was further characterized by size exclusion chromatography (SEC) using *N,N*-dimethylacetamide (DMAc) as eluent and NMR spectroscopy. Similar conditions were applied for the polymerization of cholesterol-ester-poly(DMA) and cholesterol-ketal-poly(PFPA). The latter polymer was purified by precipitation in ice cold ethanol.

In addition to poly(DMA), a fluorescently labelled derivative polymer was synthesized by copolymerization of DMA with the fluorescent monomer acryloxyethyl thiocarbamoyl rhodamine B (ARho). A DMA:ARho:CTA molar ratio of 49.5:0.05:1 was applied with identical polymerization conditions as described above.

Table S1. Characterization of fluorescently labelled polymers.

CTA	M(DMA)/M(ARho)/CTA/AIBN	Conversion [a] (%)	DP [b]	M_n^{Theor} (kDa) [b]	M_n^{SEC} (kDa) [c]	~~Đ~~ [c]
Cholesterol-ester-CTA	50/0.05/1/0.2	85	43	4.87	5611	1.08
Cholesterol-ketal-CTA	50/0.05/1/0.2	92	46	5.41	5560	1.07

[a] Determined by ^{1}H NMR analysis. [b] Calculate based on conversion and molecular weight of monomers and CTAs. [c] Determined by SEC in DMAc.

Acid-triggered cholesterol removal

Solutions at 5 mg/mL for the fluorescently labelled polymers were prepared in acetate buffer (pH= 5.5, 0.1 M) and stirred overnight at room temperature. Afterwards, the samples were dialysed against water and freeze dried. The products could then be analysed by ^{1}H-NMR and will further used for *in vitro* cell experiments.

Biolayer interferometry

Bovine serum albumin (BSA) was biotinylated by standard NHS-activated ester chemistry and dilution series (1, 2.5, 5 and 50 µg/mL) of the polymer were prepared in PBS. All solutions were transferred into black flat bottom 96 well plate which was then placed into an Octed Red96 system (Pall FortéBio). First, the streptavidin sensors were washed and a baseline in PBS was recorded for 60 s. Then, the sensors were loaded with BSA-biotin by dipping into 12.5 nM biotine-BSA (66.5 kDa) solution for 300 s. After an additional wash and baseline step, the coated sensors were dipped into the polymer solutions for 600 s to measure absorption. Next, the sensors were immersed in PBS for 600 s to measure desorption. The obtained curves were fitted and calculation of K_D values was done by the FortéBio software package.

***In vitro* cell experiments**

Dendritic cells 2.4 (DC 2.4) were cultured in RMPI medium, supplemented with 10 % fetal bovine serum (FBS), antibiotics (50 units/ml penicillin and 50 µg/ml streptomycin), 2 mM L-glutamine and 1 mM sodium pyruvate. Cells were incubated at 37 °C in a controlled and sterile environment of 95 % relative humidity and 5 % CO_2. Dendritic cells were used for all cell experiments.

Confocal microscopy

DC 2.4 cells were plated on a Willco-Dish glass bottom dishes (15 000 cells, suspended in 180 µL of culture medium) and incubated overnight. 20 µL of polymer solution (1 mg/mL) was added to the cells and cells were further incubated overnight. Subsequently, the culture medium was removed and the cells were washed with PBS and fixated in 4 % paraformaldehyde. After 15 min at 37 °C, cells were washed and 250 µL of a staining solution was added. After 30 min, the supernatants were removed and the dishes were washed with PBS prior to imaging. The staining solution (in total 1 mL PBS) was supplemented with 10 µL Hoechst stock solution (1 mg/mL in DMSO) and 5 µL of cholera toxin subunit (CTB) 488 stock solution (1 mg/mL in PBS).

Flow cytometry

DC 2.4 cells were seeded in 24-well culture plates (150 000 cells, 450 µL per well) and adhered overnight. The cells were placed on ice for 15 minutes and 50 µL of ice cold samples were added and incubated for 2 h on ice. Then, cells were washed and 0.5 mL cell dissociation buffer was added for detaching. Afterwards, cells were transferred into Eppendorf tubes, centrifugated, resuspended and

analysed by flow cytometry. The experiment was also executed at 37 °C, whereby the samples were incubated overnight at 37°C. The data were analysed by FlowJo software package.

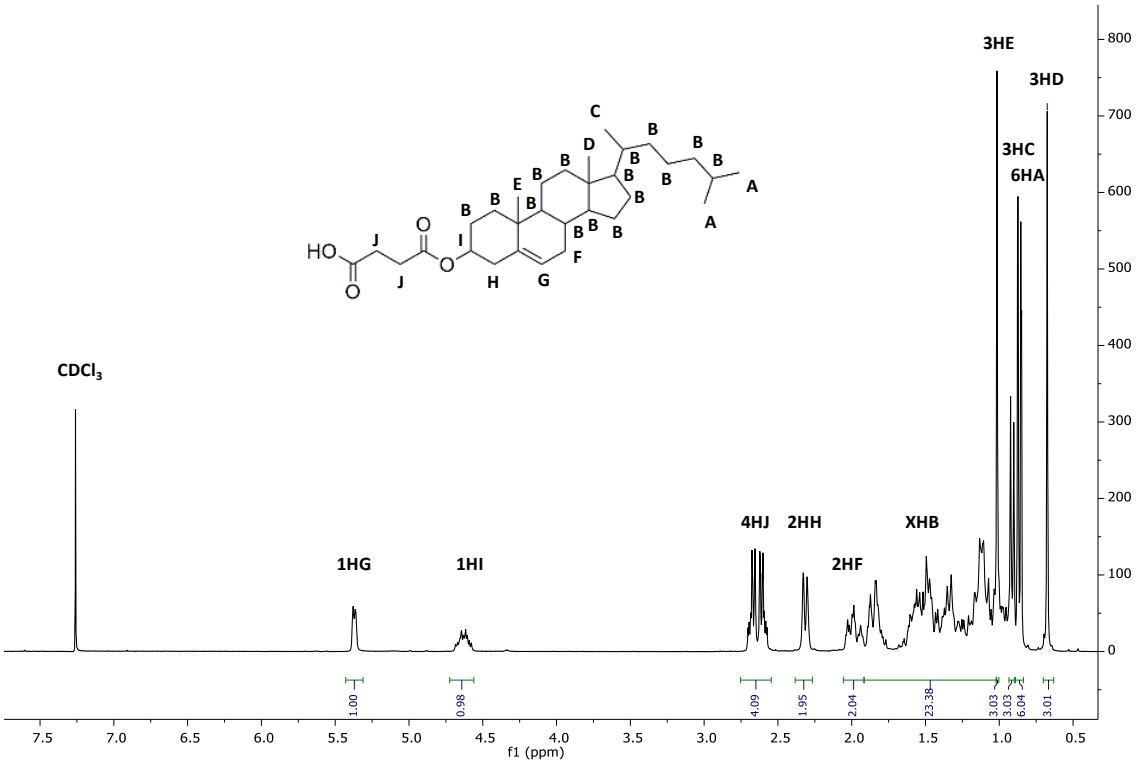

Figure S1. ^{1}H-NMR spectrum of cholesteryl hemisuccinate in $CDCl_3$.

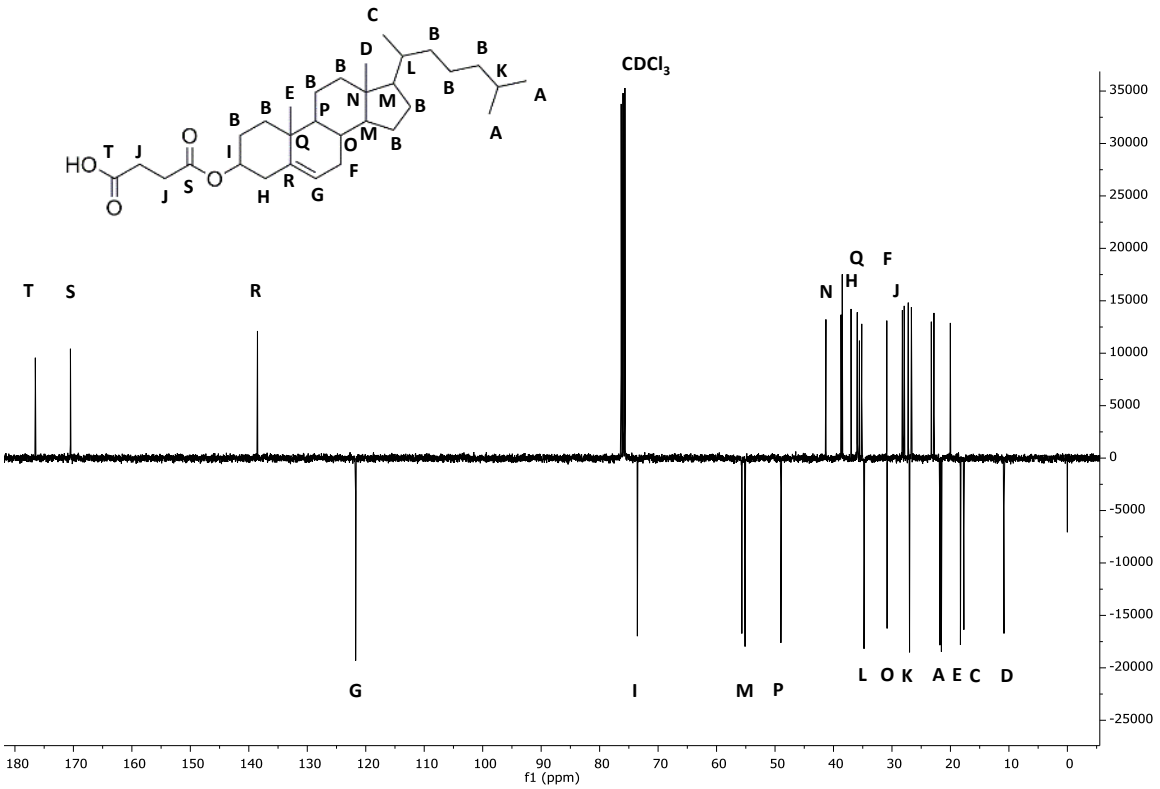

Figure S2. APT ^{13}C-NMR spectrum of cholesteryl hemisuccinate in $CDCl_3$.

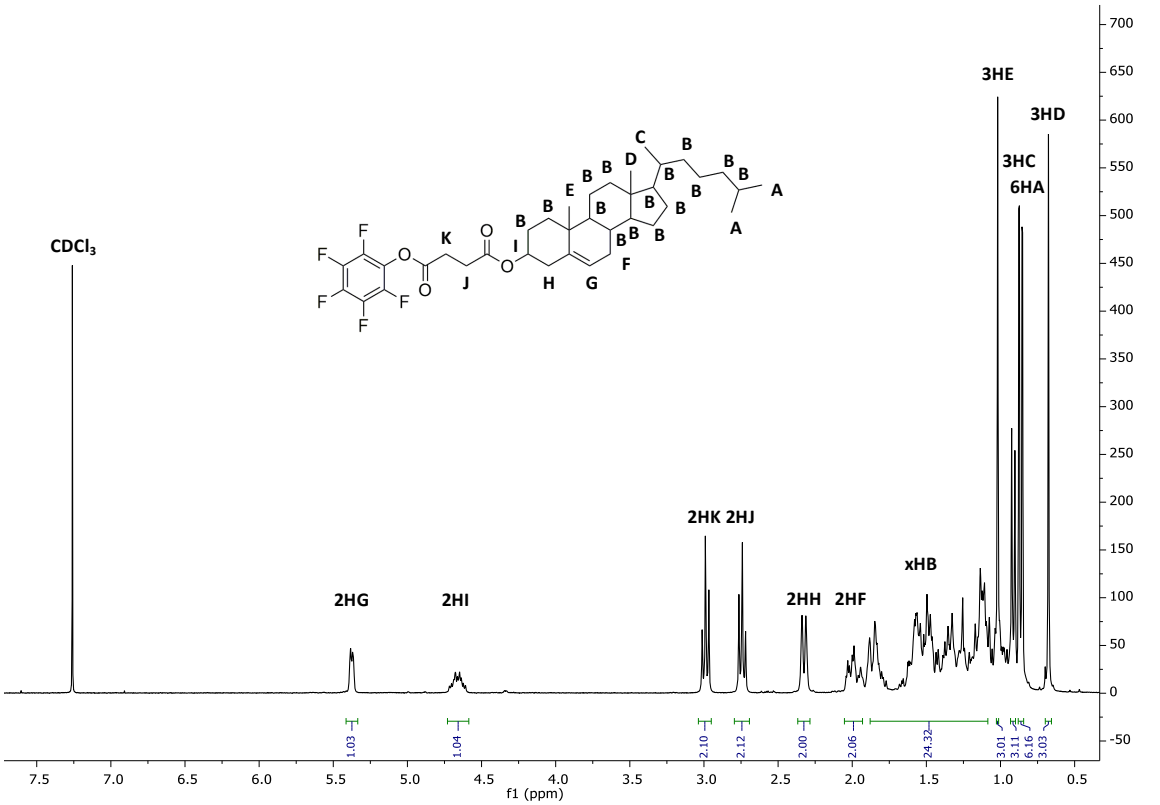

Figure S3. ^{1}H-NMR spectrum of intermediate 1 in $CDCl_3$.

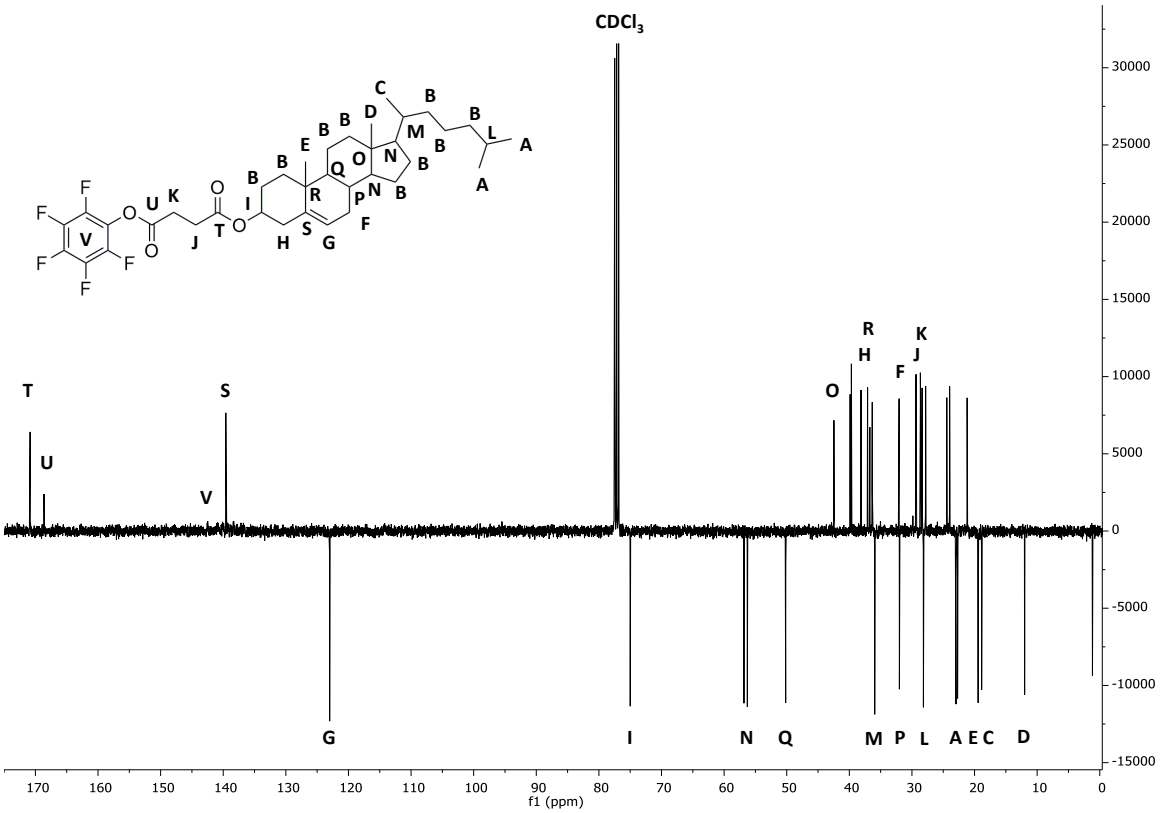

Figure S4. APT ^{13}C-NMR spectrum of intermediate 1 in $CDCl_3$.

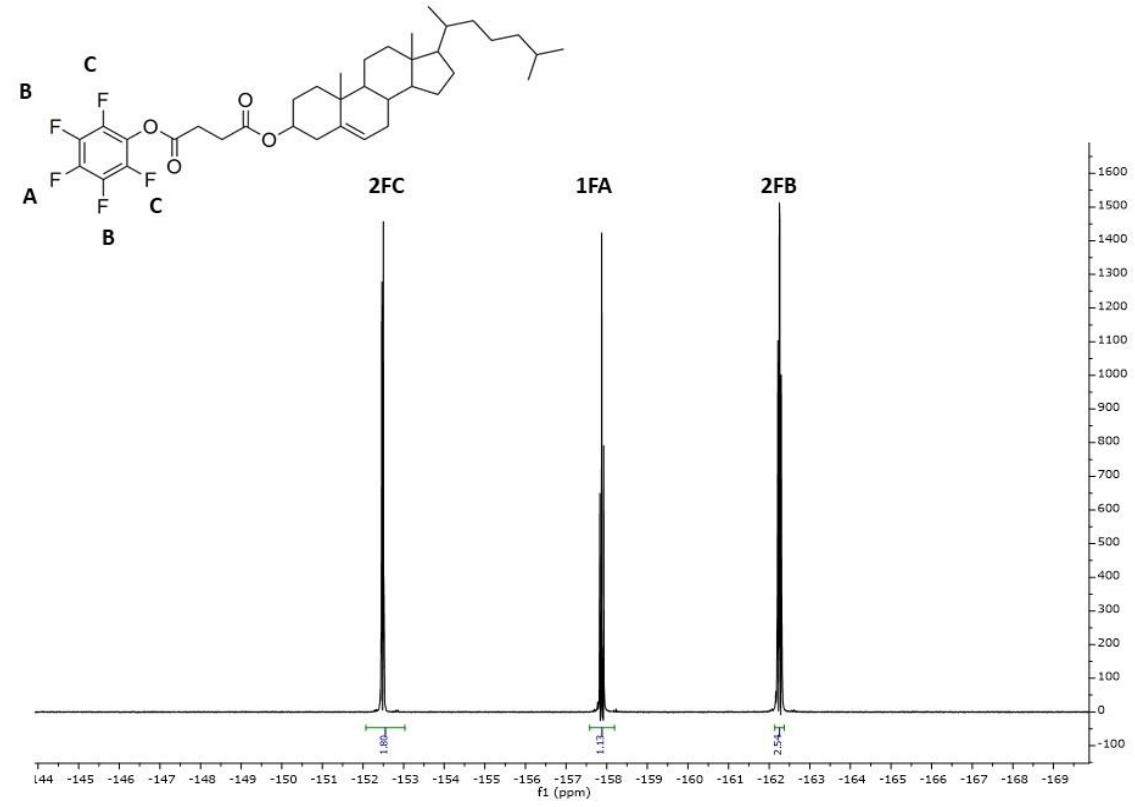

Figure S5. ^{19}F-NMR spectrum of intermediate 1 in $CDCl_3$.

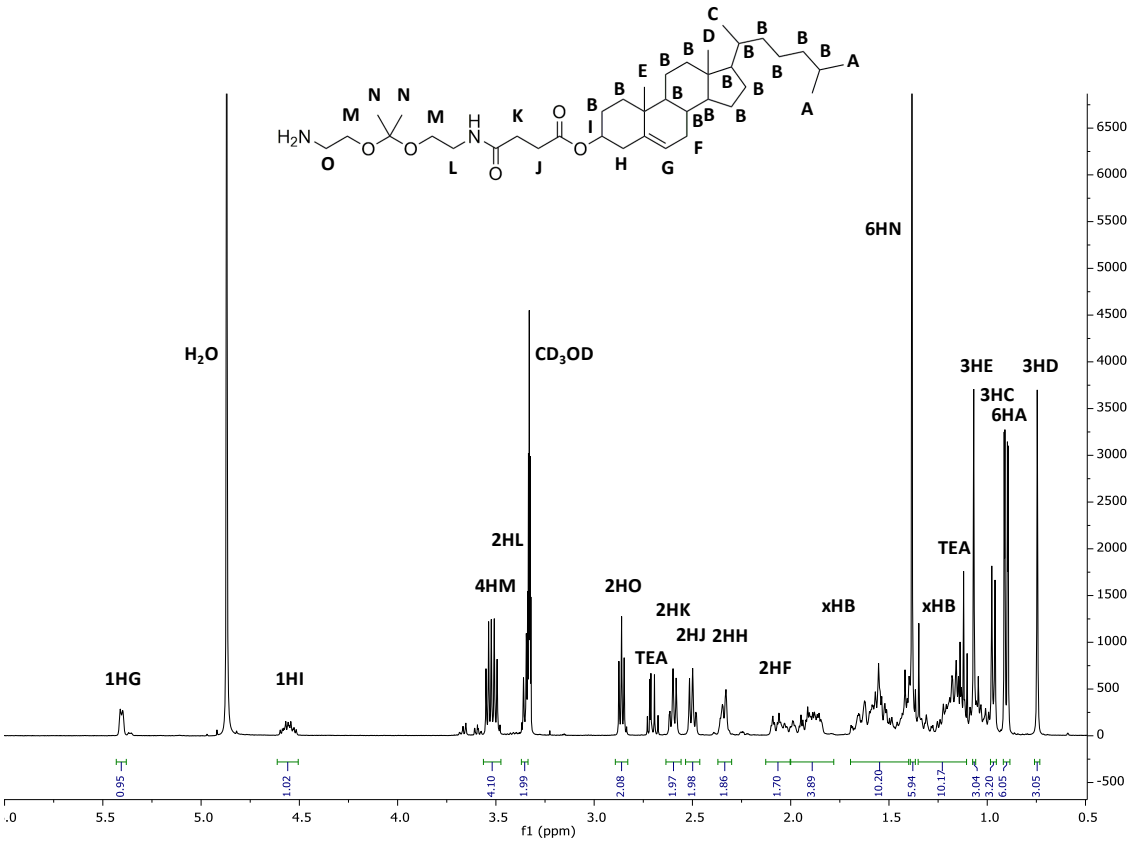

Figure S6. ^{1}H-NMR spectrum of intermediate 2 in CD_3OD.

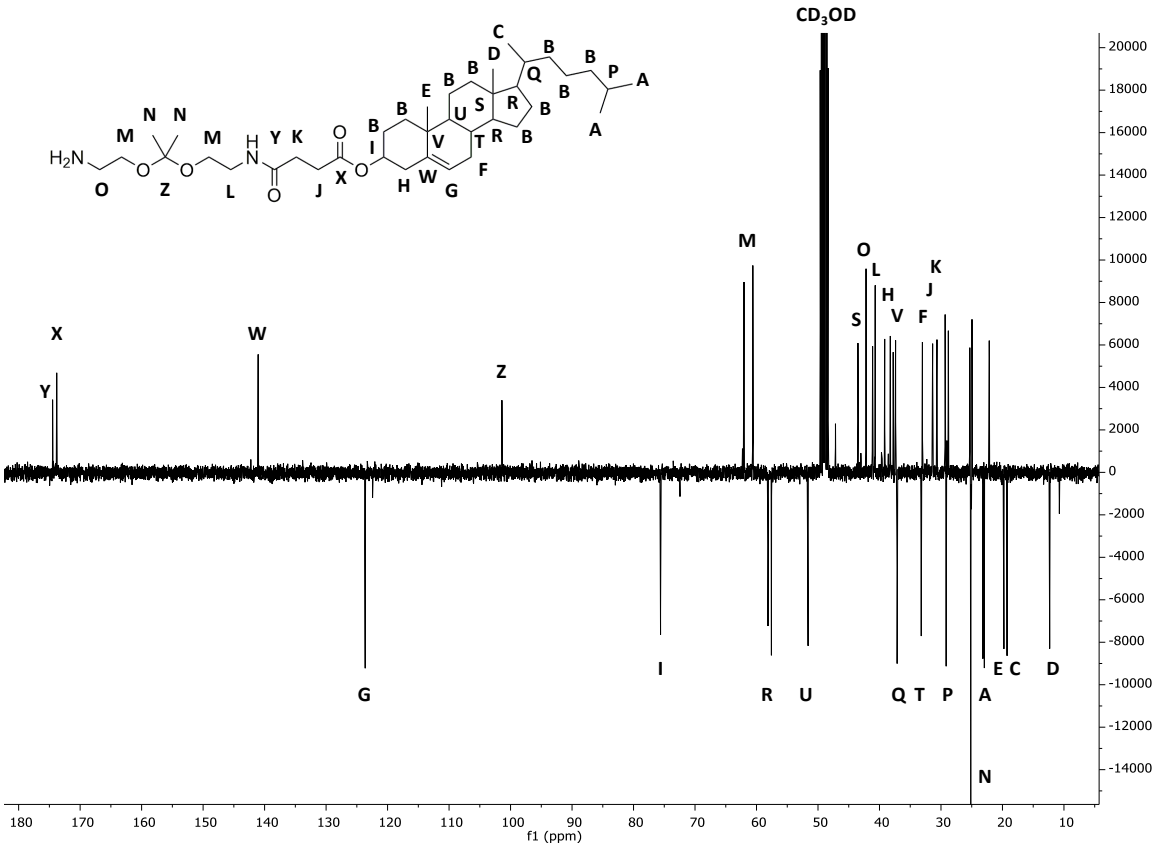

Figure S7. APT ^{13}C-NMR spectrum of intermediate 2 in CD_3OD.

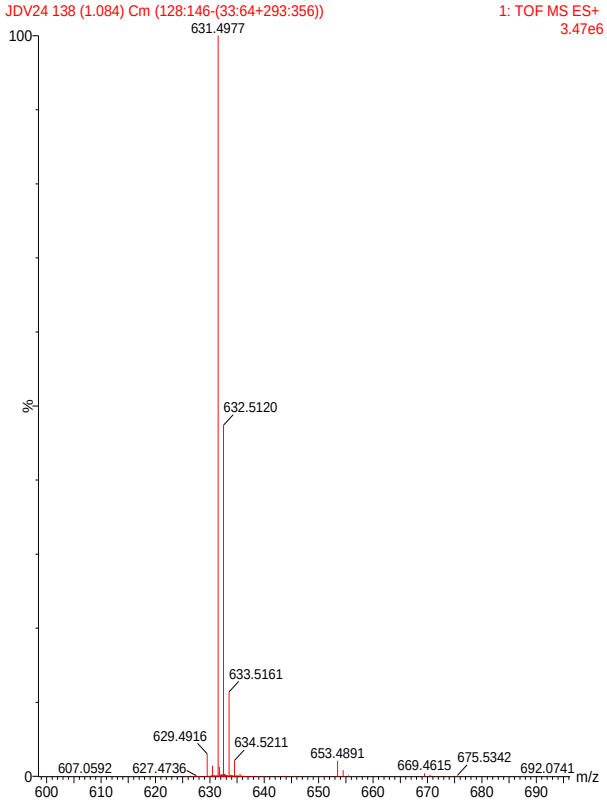

Figure S8. ESI-MS of intermediate 2.

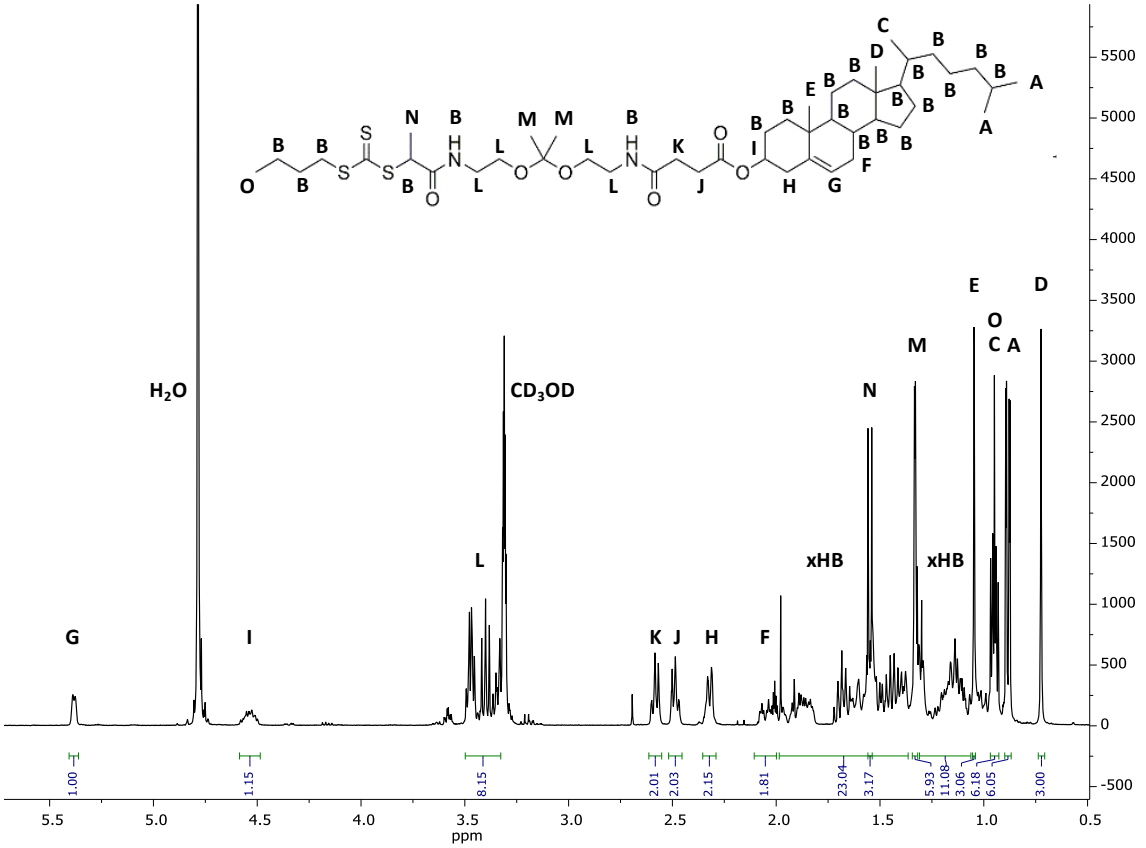

Figure S9. ^{1}H-NMR spectrum of cholesterol-ketal-CTA in CD_3OD.

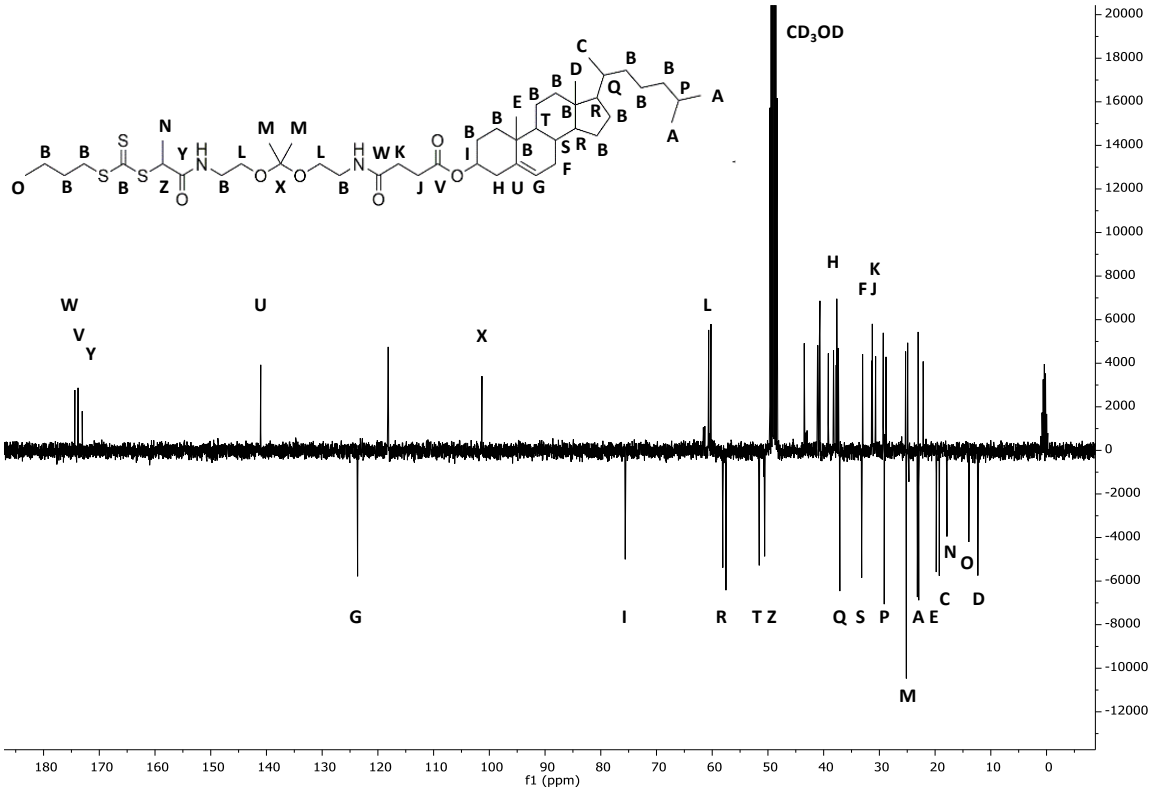

Figure S10. APT ^{13}C-NMR spectrum of cholesterol-ketal-CTA in CD_3OD.

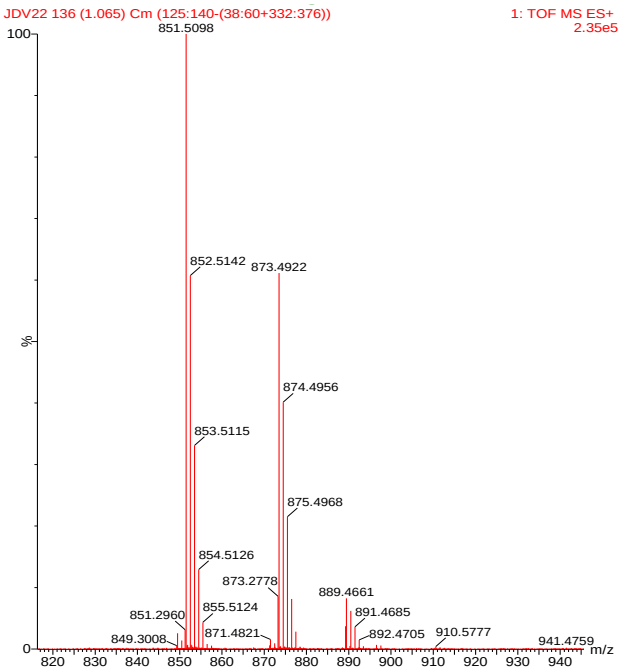

Figure S11. ESI-MS of cholesterol-ketal-CTA.

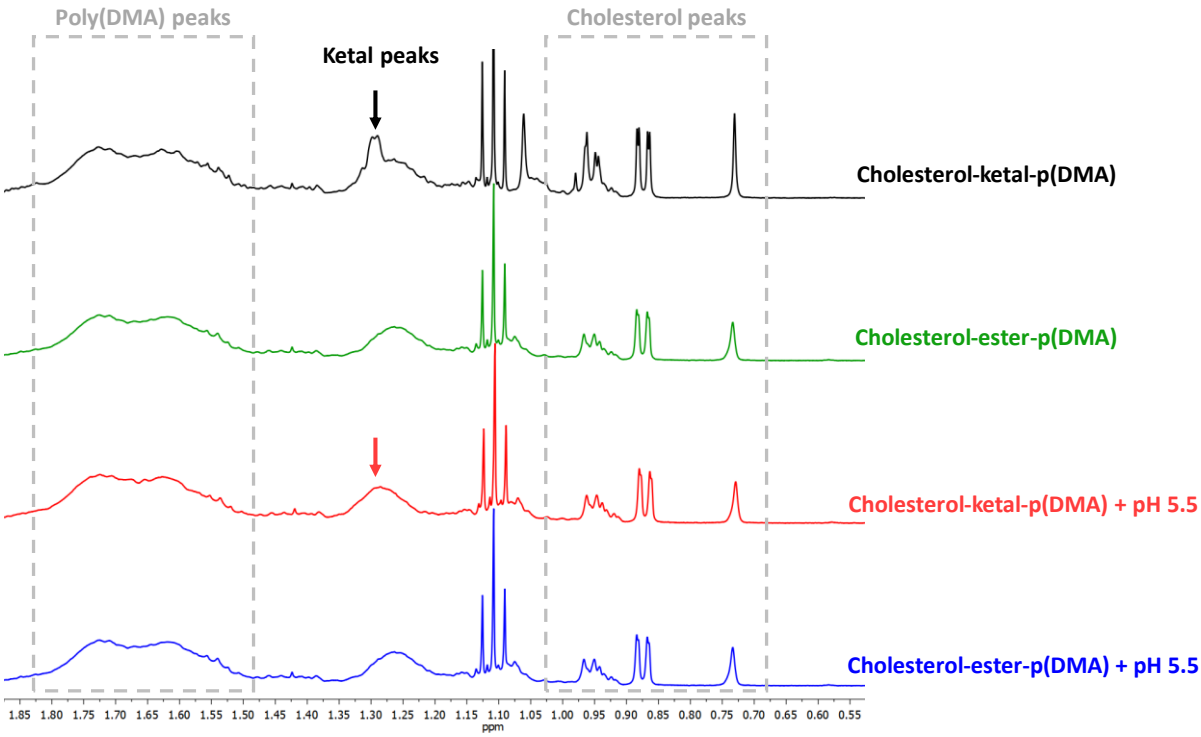

Figure S12. ^{1}H-NMR analysis: a zoomed region of the most relevant peaks before and after exposure to acidic condition.